Powder Technology 338 (2018) 67–78

Contents lists available at ScienceDirect

Powder Technology

journal homepage: www.elsevier.com/locate/powtec

Uniform and decoupled shape effects on the maximally dense random packings of hard superellipsoids

Lufeng Liu [a], Zhiyuan Yu [b], Weiwei Jin [a], Ye Yuan [a], Shuixiang Li [a,*]

[a] Department of Mechanics and Engineering Science, College of Engineering, Peking University, Beijing 100871, China
[b] Irvine Valley College, Irvine, CA 92618, USA

ARTICLE INFO

Article history:
Received 11 December 2017
Received in revised form 27 February 2018
Accepted 20 June 2018
Available online 25 June 2018

Keywords:
Superellipsoid
Order parameters
Shape effects
Maximally dense random packing

ABSTRACT

The superellipsoid model is a rich geometric model and is convenient to study the particle shape effects on random packings. The particle shape significantly influences the macroscopic and microscopic structure properties of random packings. In this work, we find uniform and decoupled shape effects on the maximally dense random packings (MDRPs) of hard superellipsoids. Slightly changing the surface shape or elongating (compressing) the particles may influence the random packing density significantly. The influences of surface shape parameter p and aspect ratio w on the random packing densities are decoupled. For the aspect ratio effects, all the packing density curves show "M" type with various p. Meanwhile, the aspect ratio effects are applicable to all the symmetric particles with three equal main cross sections when $w = 1.0$. For the surface shape effects, the packing density curve is also in "M" type with various w. The maximum of the random packing density is obtained at $p \approx 0.7$, 2.0 and $w \approx 0.7$, 1.5. Moreover, we obtain the MDRPs of hard superellipsoids via the inverse Monte Carlo packing method with a wide range of the surface shape parameter. The normalized local cubatic order parameter and a new normalized local bond-orientational order parameter are used to evaluate the order degrees of orientations and bond-orientations in random packings, respectively. The local analyses of the MDRPs of superellipsoids are carried out via the Voronoi tessellation. Two linear relationships between the mean and standard deviation of the reduced Voronoi cell volumes are obtained. Our findings should lead to a better understanding of random packings and are helpful in guiding the granular material design.

1. Introduction

Since Bernal [1] and Scott's [2] studies on the monodisperse sphere packings, the random particle packings have been applied in many fields such as the structures of liquids, glasses, heterogeneous materials and granular media [3–8]. The random packings of spherical and non-spherical particles are widely studied in decades and the particle shape significantly influences the macroscopic (microscopic) structure properties of random packings. The packing density of the Random Close Packing (RCP) of spheres is about 0.64 [1], which is close to that of the Maximally Random Jammed (MRJ) packing of spheres [9]. Previous studies demonstrate that introducing asphericity to the particle shape will change the structure properties and increase the random packing density above that of spheres. The asphericity of a particle can be increased via elongating (compressing), i.e. changing the aspect ratio, such as the spherocylinders [10–19] and ellipsoids [13, 20–27]. Meanwhile, changing the surface shape can also increase the asphericity, for example, the superballs [28]. These two shape factors are independent and fundamental in particle morphology. Therefore, systemically investigating the aspect ratio and surface shape effects on the random packings is important and meaningful.

The superellipsoid model [29] is a rich geometric model and is convenient to study the particle shape effects. It is believed that 80% of shapes of solids can be represented by superellipsoids [30, 31]. Superellipsoids are used to model symmetric particle geometries with a range of aspect ratios and edges ranging from rounded to spiky in shape [32], such as spheres, ellipsoids, superballs, and cylinder-like, cuboid-like, octahedron-like particles. The densest packing of different shaped superellipsoids has been studied by a number of researchers. For example, the densest packing of spheres is the Face-Centered Cubic (FCC) packing or Hexagonal Close Packing (HCP), which was proved by Hales in 2005 [33]. The densest known ellipsoid packings are the SM2 crystal [34] and the SQ-TR crystal [35] for different aspect ratios. The densest known superball packings are the Bravais lattices with different lattice vectors when the surface shape parameter varies [36]. Moreover, the phase behaviors of superballs were well studied by Batten et al. [37] and Ni et al. [38] The phase behaviors of spheroids [39–41] and biaxial ellipsoid [42] have also been systemically investigated.

As for the random packings of different shaped superellipsoids, the aspect ratio effects on the random packing density were not always uniform. The random packings of spheroids were studied by many

* Corresponding author.
E-mail address: lsx@pku.edu.cn (S. Li).

https://doi.org/10.1016/j.powtec.2018.06.033
0032-5910/

researchers [13, 20–27] and all their results demonstrated that the packing density reaches the maximum value when the aspect ratio is about 0.7 or 1.5 and the packing density of sphere is a local minimum, which means that slightly elongating or compressing the spheres via ellipsoids will improve the random packing density. Similarly, changing the surface shape away from spheres via superballs will also improve the random packing density, as shown by Jiao et al. in ref. [28]. Furthermore, Delaney et al. [24] and Zhao et al. [27] studied the aspect ratio effects on the random packings of superellipsoids which are elongated or compressed superballs. The random packing density curves are in "M" type when the superball is close to a sphere with the surface shape parameter $p = 5/7, 5/6, 1.0$ and 1.5. Here the shape parameter $p = m/2 = 1/\zeta$, where m is the shape parameter defined in ref. [24] and ζ is the blockiness defined in ref. [27]. However, when the superball is much closer to a cube with $p = 2.0$ and 2.5, the packing density curves are not in "M" type and the maximum value is obtained at the aspect ratio $w = 1.0$ [24, 27]. This is because their packings must be mechanically stable or jammed. The randomness must be compromised and ordered structures dominate to keep the packing structure mechanically stable or jammed when the particle shape is close to an ideal cube. In other words, the final superellipsoid packings in their work are not always on the same random degree and the aspect ratio effects are not uniform as a result of mechanical stability or jamming. Additionally, the maximal surface shape parameter p of superballs already studied is 3.0 [24, 27, 28], which is far from that of the ideal cube. The evolution of the random packings of superballs varying from sphere to cube and the maximal value on the packing density curve are still not well described. Meanwhile, the surface shape effects on the random packings of superellipsoids with different aspect ratios have not been well studied.

In order to compare the packing densities of different shaped particles in a same random state, we introduced the concept of the Maximally Dense Random Packing (MDRP) [19, 43, 44]. The MDRP is defined as the densest packing in the random state in which the particle positions and orientations are randomly distributed as quantified by specified order metrics. The packing density of the MDRP corresponds to a sharp transition in the order map, which characterizes the onset of nontrivial spatial correlations among the particles [43]. The MDRP is regarded as a glass state of hard particle systems with an artificial constraint and is always random. For particles which are good glass formers, the packing density of the MDRP is close to that of the RCP or MRJ packing, such as the MDRPs of octahedra [43] and spherocylinders [19]. However, for bad glass formers which are easy to crystalize, the MDRP is more random with lower packing density, such as the MDRPs of cuboids [44]. Two approaches have been utilized to obtain the MDRP. One is the enumeration method [19, 43], in which the MDRP is chosen as the maximally dense one among varieties of random packings already generated by common random packing algorithms. However, for bad glass formers, the enumeration method may fail to obtain the MDRP because the packing structures are easy to crystalize with common random packing algorithms. The other method is the inverse Monte Carlo packing method [44] in which the MDRP is directly generated via an artificial constraint. The artificial constraint is carried out via the order parameters and is used to prevent the presence of seed crystals or nuclei around which crystal structures form creating a solid.

In this work, we obtain the MDRPs of hard superellipsoids via the inverse Monte Carlo packing method [44] in which the formation of the local ordered structures is suppressed rigorously. The normalized local cubatic order parameter [44] and a new introduced normalized local bond-orientational order parameter are used to evaluate the local order degrees of orientations and bond-orientations, respectively. The influences of surface shape parameter p and aspect ratio w on the random packing densities are systematically investigated. As for the aspect ratio effects, all the packing density curves show "M" type with the minimal value at $w = 1.0$ and two maximal values at $w \approx 0.7, 1.5$. Meanwhile, the packing density curves also show "M" type for surface shape effects. The maximal packing density is obtained at $p \approx 0.7, 2.0$ and the minimal packing density is obtained at $p = 1.0$. Therefore, the surface shape and aspect ratio effects for superellipsoid packings are decoupled. The local analyses of the MDRPs of superellipsoids are carried out via the Voronoi tessellation [45]. Two linear relationships between the mean and standard deviation of the reduced Voronoi cell volume are obtained when the surface shape parameter $p \leq 1.5$, or $p \geq 2.0$. Our findings should lead to a better understanding of random packings.

The rest of the paper is organized as follows: in Section 2, we introduce the superellipsoid model and the overlap detection algorithm we use. Then we give the definitions of the order parameters and describe the inverse Monte Carlo packing method which is applied to generate the MDRPs. Finally, the simulation results of the MDRPs of superellipsoids are discussed in Section 3, and concluding remarks are provided in Section 4.

2. Methodology

In this part, we firstly introduce the superellipsoid model [29] and the Perram and Wertheim (PW) potential [46] used to detect overlaps between superellipsoids. Then the order parameters are proposed to evaluate the orientational and bond-orientational order degrees of superellipsoid packings, including the normalized local cubatic order parameter [44] and a new normalized local bond-orientational order parameter. Finally, we describe the inverse Monte Carlo packing method which is used to generate the MDRPs of superellipsoids.

2.1. The superellipsoid model

The superellipsoid model [29] is a rich geometric model and is convenient to study the particle shape effects. It is believed that 80% of shapes of solids can be represented by superellipsoids [30, 31]. Superellipsoids are used to model symmetric particle geometries with a range of aspect ratios and edges ranging from rounded to spiky in shape [32]. The surface function of a superellipsoid in the local Cartesian coordinates is defined as [29].

$$\left[\left(\left|\frac{x}{a}\right|\right)^{2p_0} + \left(\left|\frac{y}{b}\right|\right)^{2p_0}\right]^{\frac{p_1}{p_0}} + \left(\left|\frac{z}{c}\right|\right)^{2p_1} = 1.0 \tag{1}$$

where a, b and c are the semi-major axis lengths in the direction of x, y, and z axes, respectively, and p_0, p_1 are the surface shape parameters determining the sharpness of particle edges. The superellipsoids degenerate to ellipsoids when $p_0 = p_1 = 1.0$, and are superballs if $p_0 = p_1$, $a = b = c$. Moreover, the surface will be an ideal octahedron with $p_0 = p_1 = 0.5$, $a = b = c$ and a cube with $p_0 = p_1 = +\infty$, $a = b = c$. In this work, we focus on the random packings of superellipsoids which are elongated or compressed superballs with $a = b$ and the surface shape parameter $p = p_0 = p_1$. The aspect ratio w, which is defined as $w = c/a$, is used to describe the aspect ratio effects. Then the surface function in Eq. (1) degenerates to

$$\left(\left|\frac{x}{a}\right|\right)^{2p} + \left(\left|\frac{y}{a}\right|\right)^{2p} + \left(\left|\frac{z}{wa}\right|\right)^{2p} = 1.0 \tag{2}$$

Fig. 1 shows some typical superellipsoid examples used in this work with different p and w. The surface shape parameter p ranges from 0.7 to 5.0 with the aspect ratio w varies from 0.5 to 2.0. Meanwhile, the packings of octahedra and cuboids, two extremities of superballs with p equal to 0.5 and infinity, respectively, are also studied via the ideal polyhedral model [43]. The shapes of superellipsoids are close to octahedra when p is smaller than 1.0 and are close to cuboids when p is larger than 1.0. Meanwhile, the superellipsoids are compressed if w is smaller than 1.0 and are elongated if w is larger than 1.0, as seen in Fig. 1.

The overlap detection algorithm we use is based on the Perram and Wertheim (PW) potential introduced in ref. [46]. The generalization of

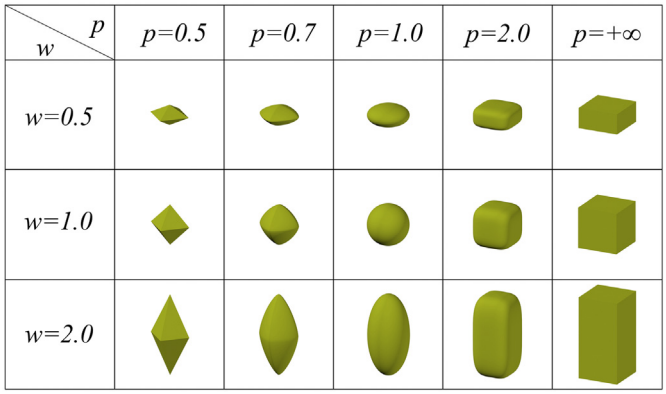

Fig. 1. Some typical superellipsoid examples used in this work with different surface shape parameter p and aspect ratio w.

the PW potential for superellipsoids can be found in ref. [38, 47]. The PW overlap potential $\zeta(A,B)$ between two particles A and B is defined through an optimization problem

$$\zeta(A,B)=\mu^2-1=\ \max_{0\le\lambda\le1}\ \min_{\vec{r}_c}\left[\lambda\zeta_A\left(\vec{r}_c\right)+(1-\lambda)\zeta_B\left(\vec{r}_c\right)\right] \quad (3)$$

where $\vec{r}_c=(x,y,z)$ is the Eulerian coordinates of a point in space, $\zeta_A(\vec{r}_c)$ and $\zeta_B(\vec{r}_c)$ are the shape functions that define the surface of particle A and B, respectively. The $\zeta_A(\vec{r}_c)$ should satisfy the following condition

$$\begin{cases}\zeta_A\left(\vec{r}_c\right)<0,\ \vec{r}_c \text{ is in particle } A\\ \zeta_A\left(\vec{r}_c\right)=0,\ \vec{r}_c \text{ is on the surface of particle } A\\ \zeta_A\left(\vec{r}_c\right)>0,\ \vec{r}_c \text{ is out of particle } A\end{cases} \quad (4)$$

For a superellipsoid particle A, the shape function is defined as

$$\zeta_A\left(\vec{r}_c\right)=\left\{\left[\left(\left|\frac{\tilde{x}}{a}\right|\right)^{2p_0}+\left(\left|\frac{\tilde{y}}{b}\right|\right)^{2p_0}\right]^{\frac{p_1}{p_0}}+\left(\left|\frac{\tilde{z}}{c}\right|\right)^{2p_1}\right\}^{\frac{1}{p_1}}-1.0 \quad (5)$$

where $(\tilde{x},\tilde{y},\tilde{z})=\boldsymbol{O}^{-1}(\vec{r}_c-\vec{r}_A)$ are the relative coordinates of $\vec{r}_c$ with respect to the particle A centered at $\vec{r}_A=(x_0,y_0,z_0)$ with the reference orientation matrix $\boldsymbol{O}=[\vec{e}_1,\vec{e}_2,\vec{e}_3]$. Here $\vec{e}_1,\vec{e}_2,\vec{e}_3$ is the directions of the three main axes of particle A.

The μ in Eq. (3) is the scaling factor which means that the particles A and B will be in external tangency at the point $\vec{r}_c^{\,o}$ if they are rescaled by $\mu=\sqrt{1+\zeta(A,B)}$ with their positions and orientations unchanged. Here $\vec{r}_c^{\,o}$ is the optimal solution of $\vec{r}_c$. $\mu=1$ means that the particles A and B are just externally tangent and A, B need not to be enlarged or shrunk. In a similar way, $\mu>1$ means that the particles A, B need to be enlarged to make them externally tangent, i.e. they are originally disjoint. $\mu<1$ means that the particles A, B need to be shrunk to make them externally tangent, i.e. they are originally overlapping. The overlap detecting samples of two particles A and B with $\mu<1$, $\mu=1$ and $\mu>1$ are shown in Fig. 2(a), (b) and (c), respectively. Therefore, the sign of $\zeta(A,B)$ gives us an overlap criterion

$$\begin{cases}\zeta(A,B)<0, \text{if } A \text{ and } B \text{ are overlapping}\\ \zeta(A,B)=0, \text{if } A \text{ and } B \text{ are externally tangent}\\ \zeta(A,B)>0, \text{if } A \text{ and } B \text{ are disjoint}\end{cases} \quad (6)$$

In this work, the PW overlap potential $\zeta(A,B)$ in Eq. (3) is calculated via the Newton–Raphson (NR) method with the first initial solution $\vec{r}_{c0}=(\vec{r}_B+\vec{r}_A)/2$ and $\lambda=0.5$. If the result for the first initial solution is not convergent, another initial solution with a fluctuation at $\vec{r}_{c0}$ is chosen until the result is convergent. The NR method works well for the superellipsoids we studied and its details can be found in ref. [38, 47].

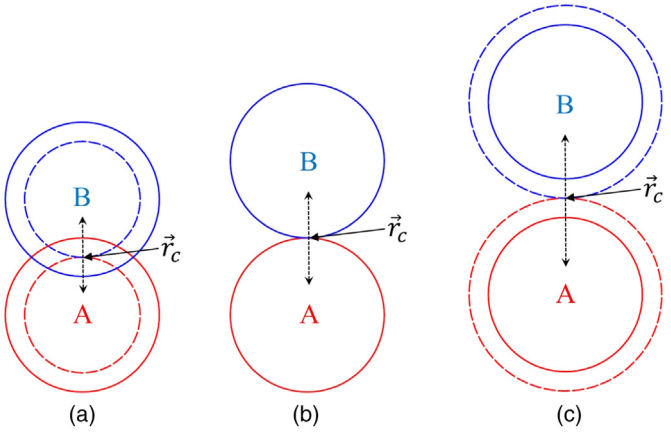

Fig. 2. Illustration of the scaling factor μ in the PW overlap potential. (a) $\mu<1$, $\zeta(A,B)<0$, A and B are overlapping. (b) $\mu=1$, $\zeta(A,B)=0$, A and B are externally tangent. (c) $\mu>1$, $\zeta(A,B)>0$, A and B are disjoint.

2.2. The order parameters

2.2.1. The normalized local cubatic order parameter

The normalized local cubatic order parameter $\tilde{S}_{4local}$ is based on the cubatic order parameter S_4 defined by Batten et al. [37] and is used to evaluate the local cubatic order degree of the packings of symmetrical particles with three axes [44]. The average orientation correction of particles with n nearest neighbor particles is evaluated by $S_{4local,\,n}$ which is defined as

$$S_{4local,n}=\frac{1}{N}\sum_{i=1}^{N}\ \max_j\left[\frac{1}{14n}\sum_{k=1}^{n}\sum_{l=1}^{3}\left(35\cos^4\theta_{ij,kl}-30\cos^2\theta_{ij,kl}+3\right)\right] \quad (7)$$

where N is the total number of particles in the packing system, $n=1, 2, 3\ldots, 26$ represents the number of particles which are closest to the ith particle, j, $l=1, 2, 3$ are the three main axes of particles. $\cos\theta_{ij,kl}=|\vec{u}_{ij}\cdot\vec{u}_{kl}|$ with $\vec{u}_{ij}$ the ith central particle's jth axis and $\vec{u}_{kl}$ the lth axis of the kth neighbor particle of the ith central particle. We note that there are 26 neighbor particles around a particle in the simple cubic lattice packing of cubes and 26 is the maximal number of the neighbor particles in superellipsoid packings we studied. In order to use a universal way to evaluate the local order degree for all superellipsoid packings, we choose 26 as the maximal number of n. Moreover, 26 is large enough to control the local cubatic order in superellipsoid packings. We have verified that if the 26 local cubatic order parameters $S_{4local,\,n}$ are small enough, the values of $S_{4local,\,27}$, $S_{4local,\,28}$, $S_{4local,\,29}$ and so on are very small as well.

The values of $S_{4local,\,n}$ in the random state are calculated via the Monte Carlo tests [44] and are found in Gaussian distributions. The means $S^{\mu}_{4local,\,n}$ and standard deviations $S^{\sigma}_{4local,\,n}$ are linear to $1/\sqrt{n}$ and $1/\sqrt{Nn}$, respectively

$$\begin{cases}S^{\mu}_{4local,n}=0.30972/\sqrt{n}\\ S^{\sigma}_{4local,n}=0.38720/\sqrt{Nn}\end{cases} \quad (8)$$

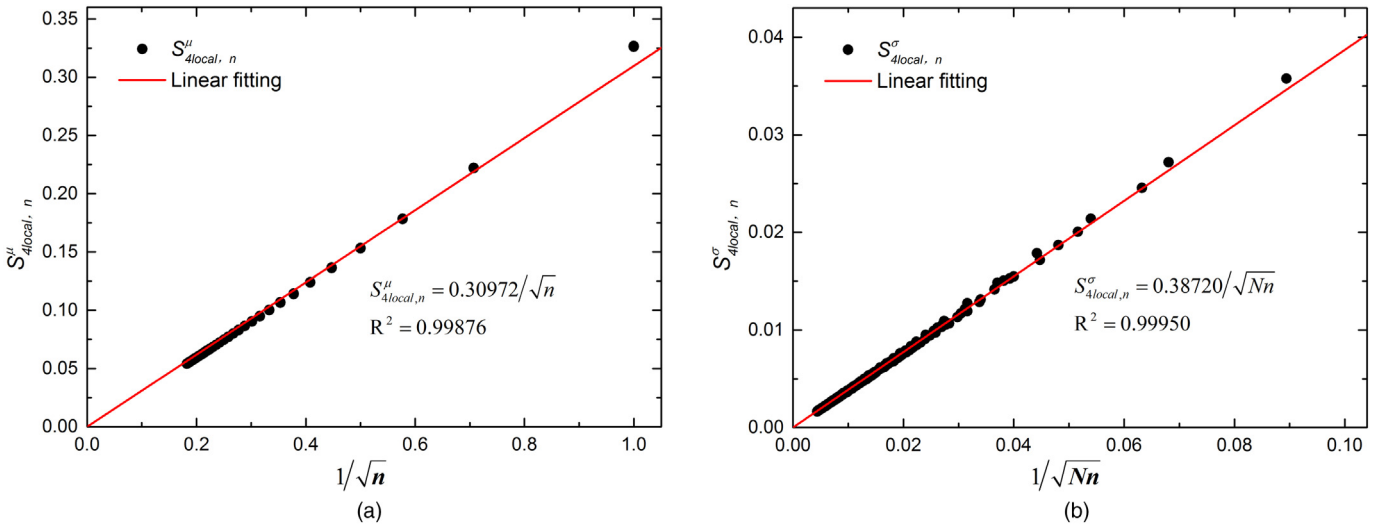

Fig. 3. (a) The relationship between the means $S^{\mu}_{4local,\ n}$ and the number of nearest neighbors n for different particle amount N. The $S^{\sigma}_{4local,\ n}$ is proportional to $1/\sqrt{n}$ with a slope 0.30972 and is not related to N. The correlation factor of the fitted line is $R^2 = 0.99876$. (b) The relationship between the standard deviations $S^{\sigma}_{4local,\ n}$ and the number of nearest neighbors n for different particle amount N. The $S^{\sigma}_{4local,n}$ is proportional to $1/\sqrt{Nn}$ with a slope 0.38720. The correlation factor of the fitted line is $R^2 = 0.99950$.

as shown in Fig. 3(a) and (b). Then the $\tilde{S}_{4local,n}$ is normalized as

$$\tilde{S}_{4local,n} = \left| \frac{S_{4local,n} - S^{\mu}_{4local,n}}{S^{\sigma}_{4local,n}} \right| \tag{9}$$

and the normalized local cubatic order parameter $\tilde{S}_{4local}$ is

$$\tilde{S}_{4local} = \max_n \left\{ \tilde{S}_{4local,n} | n = 1, 2, 3..., 26 \right\}. \tag{10}$$

For a perfectly ordered lattice packing of particles with three axes, both the S_4 and $S_{4local,\ n}$ are unity. However, in a quasi-random packing [48] with large amounts of local ordered clusters, the S_4 is small while the $\tilde{S}_{4local}$ is very large. In a random packing with no obvious global or local orientational order, both the S_4 and $\tilde{S}_{4local}$ are small.

2.2.2. The normalized local bond-orientational order parameter

The normalized local bond-orientational order parameter $\tilde{Q}_{6local}$ is similar to the original bond-orientational order parameter Q_6 [49], which is an important order parameter when describing glass transitions [50–52] and crystalline clusters [53–55]. The Q_6 is calculated as follows [49, 56].

$$Q_6 = \sqrt{\frac{4\pi}{13} \sum_{m=-6}^{m=6} \left| \frac{1}{N_b} \sum_{i=1}^{N_b} Y_{6m}(\theta_i, \varphi_i) \right|^2} \tag{11}$$

where N_b is the total number of neighbor bonds of all particles in the system, θ_i and φ_i are the polar and azimuthal angles of bond i, $Y_{lm}(\theta,\varphi)$ are the spherical harmonics. A set of methods are used to judge whether two particles are neighbors [57]. However, the value of Q_6 is infinitesimally small in a random packing system while the exact value varies slightly depending on the definition of neighbors.

In order to evaluate the average bond-orientation correction of particles with n nearest neighbor particles, the local bond-orientational order parameter $Q_{6local,\ n}$ is introduced as

$$Q_{6local,n} = \sqrt{\frac{4\pi}{13} \sum_{m=-6}^{m=6} \left| \frac{1}{N} \sum_{i=1}^{N} \left[\frac{1}{n} \sum_{j=1}^{n} Y_{6m}\left(\theta_{ij}, \varphi_{ij}\right) \right] \right|^2} \tag{12}$$

where N is the total number of particles in the packing system, n represents the number of the nearest neighbor particles of the ith particle, θ_{ij}, φ_{ij} are the polar and azimuthal angles of the bond formed by particle i and j. Here we choose $n = 1, 2, 3..., 26$ to evaluate the bond-orientational order degrees of different sized local structures around the ith particle. We also choose 26 as the maximal number of n for the reasons mentioned in Section 2.2.1.

The values of $Q_{6local,\ n}$ in a random system with limited particle amount cannot accurately be zero due to the limited particle amount N and the number of nearest neighbors n. Therefore, the Monte Carlo test [19, 43, 44] is introduced to evaluate the values of $Q_{6local,\ n}$ in the random state. For each $n \in \{1,2,3...,26\}$, $N \cdot n$ unit vectors with random directions are uniformly generated in the space, representing the total bonds used to calculate $Q_{6local,\ n}$ in a packing system with N particles. Then the $Q_{6local,\ n}$ is calculated as Eq. (12). Finally, the test is repeated 10,000 times and the results are shown in Fig. 4.

Fig. 4(a) shows the probability distribution of $Q_{6local,\ 1}$ over 10,000 samples with $N = 1000$. The distribution is fitted by a Gaussian distribution function with the correlation factor $R^2 = 0.998$. The mean $Q^{\mu}_{6local,\ 1}$ and standard deviation $Q^{\sigma}_{6local,\ 1}$ calculated from the fitted Gaussian distribution are 0.03068 and 0.00611, respectively. Meanwhile, the results of $Q_{6local,\ 26}$ are shown in Fig. 4(b) with $Q^{\mu}_{6local,\ 26} = 0.00603$, $Q^{\sigma}_{6local,\ 26} = 0.00123$, and $R^2 = 0.997$. The values of $Q_{6local,\ n}$ for other N and n are in Gaussian distributions as well. Moreover, we find that both the mean $Q^{\mu}_{6local,\ n}$ and standard deviation $Q^{\sigma}_{6local,\ n}$ are linear to $1/\sqrt{Nn}$ with

$$\begin{cases} Q^{\mu}_{6local,n} = 0.98123/\sqrt{Nn} \\ Q^{\sigma}_{6local,n} = 0.19379/\sqrt{Nn} \end{cases} \tag{13}$$

as shown in Fig. 4(c) and (d). Then the $\tilde{Q}_{6local,n}$ is normalized as

$$\tilde{Q}_{6local,n} = \left| \frac{Q_{6local,n} - Q^{\mu}_{6local,n}}{Q^{\sigma}_{6local,n}} \right| \tag{14}$$

and the normalized local bond-orientational order parameter $\tilde{Q}_{6local}$ is

$$\tilde{Q}_{6local} = \max_n \left\{ \tilde{Q}_{6local,n} | n = 1, 2, 3..., 26 \right\} \tag{15}$$

The $\tilde{Q}_{6local}$ is large in an ordered packing and is small in a random packing.

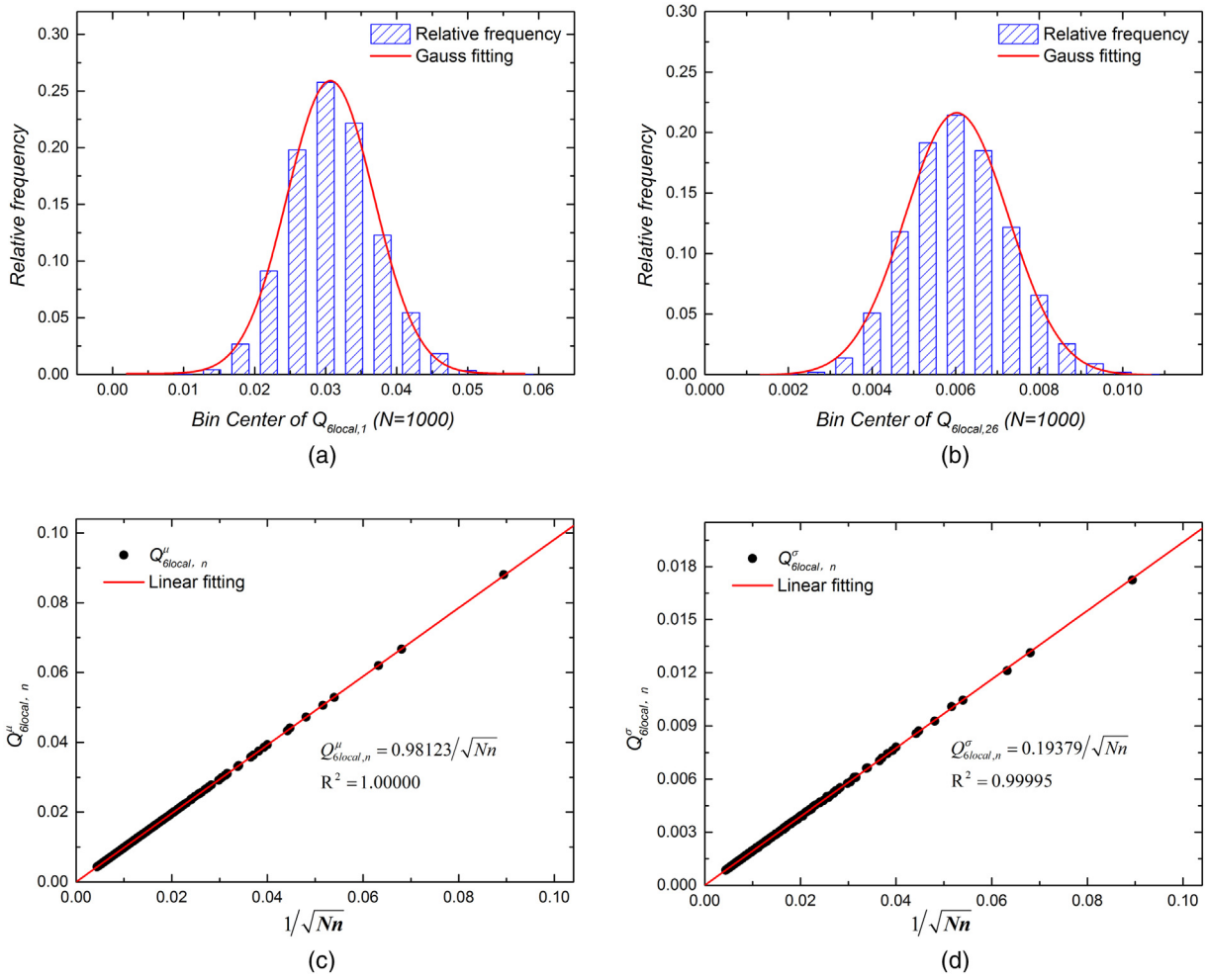

Fig. 4. (a) Histograms of the relative frequency of $Q_{6local,\,1}$ over 10,000 samples with $N = 1000$. The data are fitted by a Gaussian distribution with $Q^{\mu}_{6local,\,1} = 0.03068$, $Q^{\sigma}_{6local,\,1} = 0.00611$ and $R^2 = 0.998$. (b) Histograms of the relative frequency of $Q_{6local,\,26}$ over 10,000 samples with $N = 1000$. The data are fitted by a Gaussian distribution with $Q^{\mu}_{6local,\,26} = 0.00603$, $Q^{\sigma}_{6local,\,26} = 0.00123$ and $R^2 = 0.997$. (c) The relationship between the mean $Q^{\mu}_{6local,\,n}$ and the number of nearest neighbors n for different particle amount N. The $Q^{\mu}_{6local,\,n}$ is proportional to $1/\sqrt{Nn}$ with a slope 0.98123 and $R^2 = 1.00000$. (d) The relationship between the standard deviation $Q^{\sigma}_{6local,\,n}$ and the number of nearest neighbors n for different particle amount N. The $Q^{\sigma}_{6local,\,n}$ is proportional to $1/\sqrt{Nn}$ with a slope 0.19379 and $R^2 = 0.99995$.

2.3. The inverse Monte Carlo packing method

The inverse Monte Carlo packing method [44] based on stochastic optimization allows one to generate maximally dense packing configurations of hard particles with a controllable degree of order/disorder quantified via prescribed order parameters. This method is based on the adaptive shrinking cell (ASC) method [58, 59]. In the inverse Monte Carlo packing method, the particles are randomly translated or rotated. The boundary of the packing system is fixed to be cubic with periodical boundary conditions in three directions and is allowed to compress but not shear. Besides the non-overlapping condition, the particle movement and boundary deformation are also rejected if the calculated order parameters are larger than the prescribed values, which is regarded as an artificial constraint. The prescribed values of order parameters are set to be small enough to prevent the presence of seed crystals or nuclei around which crystal structures form creating a solid. Therefore, the crystallization is inhibited and the system becomes a supercooled liquid and turns into glass. Meanwhile, the packing configuration is compressed as slow as possible to make the finial packing maximally dense. Finally, we generate a MDRP which is the maximally dense packing in the random state. Here we use the normalized local cubatic order parameter $\tilde{S}_{4local}$ and the normalized local bond-orientational order parameter $\tilde{Q}_{6local}$ introduced above to control the local order degrees of orientations and bond-orientations, respectively.

At the beginning of a common slow compression progress, the packing density can be increased rapidly while the packing structure maintaining very random with the order parameters approach to zero. Then the further increase of packing density must be accompanied with the increase of order parameters. Therefore, the packing density of the MDRP corresponds to a sharp transition on the upper bound of the order map [19, 43], which characterizes the onset of nontrivial spatial correlations among the particles.

In the inverse Monte Carlo packing method used in this work, the packing configuration is compressed as slow as possible to make the finial packing maximally dense. However, the packing configuration cannot be further compressed because the prescribed values of order parameters for acceptance is 0.5, which is very small and efficiently controls the order degree of the packing configurations [44], and the exact values of order parameters $\tilde{S}_{4local}$ and $\tilde{Q}_{6local}$ are about 0.5 with a few simulation errors smaller than 0.01. The packing density of the final packing configuration corresponds to the upper bound when the order parameters are equal to 0.5 in the order map. The final packing is the MDRP of superellipsoids on a same random degree evaluated by the order parameters. Therefore, all the packings we generated via the inverse Monte Carlo packing method are in the same random state and the exact values of order parameters $\tilde{S}_{4local}$ and $\tilde{Q}_{6local}$ are all about 0.50 with a few simulation errors smaller than 0.01. More details can be seen in ref. [44].

We note that previous works [43, 44] show that size effect on the packing density is negligible if the total particle number is larger than 125. Meanwhile, the computational cost increases rapidly as the particle number increases. As a compromise between accuracy and computational cost, we chose the particle number N to be 200.

3. Results and discussion

As mentioned above, we generate the MDRPs of superellipsoids via the inverse Monte Carlo packing method. All the results of superellipsoids are averaged over 4 times and the error bars in Fig. 6 and Fig. 7(a), (b) represent the standard deviations. Some finial packing configurations with 200 superellipsoids are shown in Fig. 5. All the packings are very random with the order parameters $\tilde{S}_{4local}$ and $\tilde{Q}_{6local}$ smaller than 0.5. The packing densities of the MDRPs of superballs and superellipsoids are demonstrated below and the microscopic properties are analyzed via the Voronoi tessellation [45].

3.1. The MDRPs of superballs

The packing densities of superballs with different surface shape parameter p are shown in Fig. 6 and are compared with the literature results. The packings generated by Jiao et al. are in the state of MRJ, while the packings generated by Delaney [24] and Zhao [27] may not be in the same state, some of them are random and others are ordered. We obtain the MDRPs of superballs with a wider range ($0.7 \le p \le 5.0$) of the surface shape parameter p. The packing density curve of the MDRPs is in "M" type with the minimum at $p = 1.0$ and two maximums at $p \approx 0.7, 2.0$. The packing densities of the MDRP of spheres ($p = 1.0$) and octahedra ($p = 0.5$) are 0.644 and 0.701, respectively, which are similar to those of the RCPs [1] or MRJs [9, 60] with no frictions. We note that both the sphere and octahedron are good glass formers. Meanwhile, the packing density of the MDRP of cubes ($p = +\infty$) is 0.642, lower than 0.734 which is the packing density of the ideal jamming point of cubes at zero shear stress with abundant small ordered clusters obtained by Smith et al. [61]. While the MRJ of cubes is still not obtained or ever not exist [60] and the packing density of the RCP of cubes generated by different methods varies significantly with different order degrees [62–64]. This is because cube is easy to crystalize and is not a good glass former.

As shown in Fig. 6, the packing densities of the MDRPs are similar to the other results when $p \le 1.5$, which means that all these superballs are good glass formers. However, the MDRPs are more random with lower packing density when p is larger than 1.5. This is because the superballs with large p are not good glass formers and their packings are easy to crystallize, as discussed by Delaney et al. in ref. [24]. The inserts in Fig. 6 show the packing configurations of superballs with $p = 2.5$ for MDRP and MRJ [28], respectively. The MRJ packing configuration with $p = 2.5$ is obtained via the adaptive shrinking cell (ASC) method [58, 59] and is similar to that generated via the DTS algorithm in ref. [28]. The MDRP configuration is random without obvious local or global order structures but may not be mechanically stable or jammed. However, small ordered clusters having three to four particles are abundant in the MRJ packing while no obvious global order structures are observed, as can be seen in the insert of Fig. 6. Moreover, the packing configuration of superballs with $p = 2.5$ generated by Delaney et al. is globally ordered, which is shown in Fig. 3(d) in ref. [24].

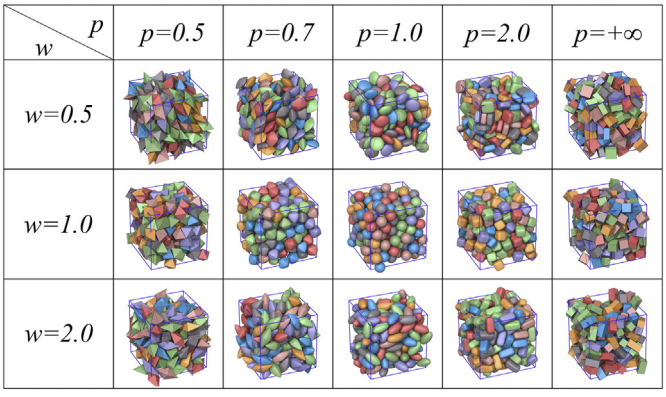

Fig. 5. The packing configurations of 200 superellipsoids with different surface shape parameter p and aspect ratio w. All the packings are very random with the order parameters $S_{\sim 4local}$ and $Q_{\sim 6local}$ smaller than 0.5.

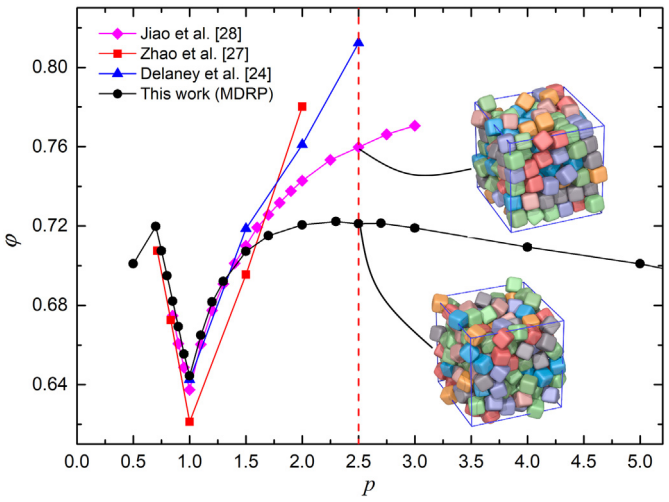

Fig. 6. The relationship between the packing densities φ of the MDRPs of superballs and the surface shape parameter p. The results are compared with literature results. The packing density curve of the MDRPs is in "M" type with the minimum at $p = 1.0$ and two maximums at $p \approx 0.7, 2.0$, respectively. For $p \le 1.5$, the MDRPs is similar to the other results. However, the MDRPs is more random with lower packing density when p is much larger. The insets show the packing configurations of the MDRP and MRJ, respectively, with $p = 2.5$.

3.2. The MDRPs of superellipsoids

The effects of aspect ratio w on the packing densities of the MDRPs of superellipsoids are shown in Fig. 7. All the packing density curves are in "M" type with the minimum at $w = 1.0$ and two maximums at $w \approx 0.7, 1.5$. Fig. 7(a) and (b) show the packing densities of the MDRPs of superellipsoids with $p \le 1.0$ and $p \ge 1.0$, respectively. For $p = 0.5$, the superellipsoids are ideal octahedra and the random packing density changes little when w varies from 0.7 to 1.5. The distinction between the minimum and maximums in the "M" type is quite small. When p varies from 0.7 to 1.0, the packing density curve moves down and keeps the "M" type. When p is larger than 1.0, the packing density curve still keeps the "M" type. However, the packing density curve firstly moves up and reaches the top at $p \approx 2.0$. Then the packing density curve moves down until $p = +\infty$ for which the superellipsoids are cuboids.

The MDRPs of superellipsoids with $p = 1.0, 1.5, 2.0$ and 2.5 are compared to literature results in Fig. 7(c), (d), (e) and (f), respectively. When $p = 1.0$, the superellipsoids degenerate to ellipsoids and all the packing curves obtained by the researchers are in "M" type. The packing density curve of the MDRPs is almost the same as the results of Delaney et al. [24] and Donev et al. [22] which were obtained via the algorithms based on the Lubachevsky-Stillinger (LS) algorithm [65]. While the results of Zhou et al. [25] and Zhao et al. [27] are slightly lower, because they used the algorithms based on the particle depositing packing method. When $p = 1.5$, the packing density curve of the MDRPs is similar to that of Delaney et al.'s work [24] except the minimum value at $w = 1.0$. The packing density of the MDRP with $p = 1.5$, $w = 1.0$ is a little

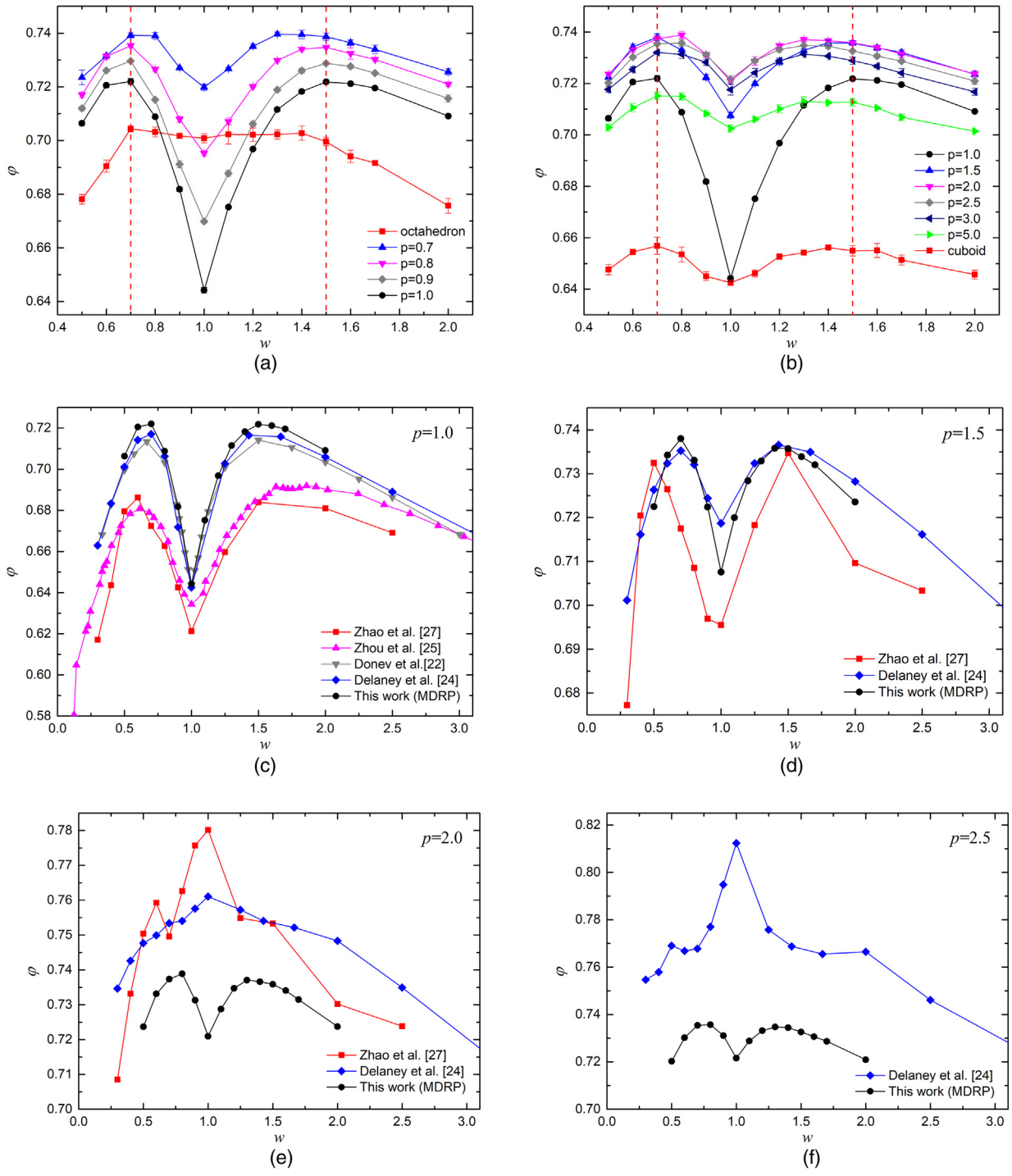

Fig. 7. (a) The relationships between the packing densities φ of the MDRPs and the aspect ratio w with the surface shape parameter $p = 0.5, 0.7, 0.8, 0.9$ and 1.0. (b) The relationships between the packing densities φ of the MDRPs and the aspect ratio w with the surface shape parameter $p = 1.0, 1.5, 2.0, 2.5, 3.0, 5.0$ and $+\infty$. (c-f) The packing density curves of the MDRPs with $p = 1.0$,1.5,2.0 and 2.5 are compared to literature results in (c), (d), (e) and (f), respectively.

smaller than that of Delaney et al.'s work [24]. This is because the order degree of the superellipsoid packing with $p = 1.5$, $w = 1.0$ obtained by Delaney et al. is a little higher, as described in ref. [24]. The packing density curves of the MDRPs are still in "M" type when $p = 2.0$ and 2.5. However, the packing density curves in Delaney and Zhao's work are not in "M" type any longer and are higher than those of the MDRPs. Their only maximum values are obtained at $w = 1.0$, where the superellipsoids are superballs which are much closer to ideal cubes. This is because their packings must be mechanically stable or jammed. The randomness must be sacrificed and order structures dominate to keep the packing mechanically stable or jammed when the particle shape is close to an ideal cube. Therefore, the final packings of superellipsoids in their work are not always in the same random state and the aspect ratio effects are not uniform as a result of mechanical stability or jamming.

We also investigate the surface shape effects on the MDRPs of superellipsoids. Fig. 8 shows the relationship between the surface shape parameter p and the random packing densities of superellipsoids with different aspect ratio w. All the packing density curves show "M" type with the minimum at $p = 1.0$ and two maximums at $p \approx 0.7$, 2.0. We conclude that for the aspect ratio effects, all the packing density

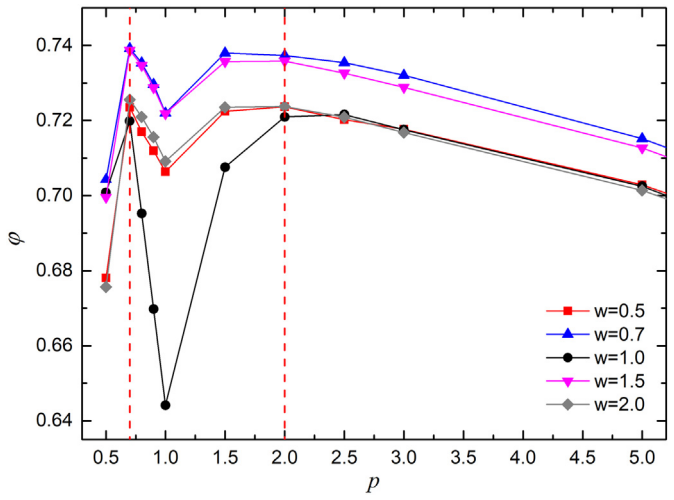

Fig. 8. The relationship between the surface shape parameter p and the random packing densities of superellipsoids with the aspect ratio $w = 0.5, 0.7, 1.0, 1.5$ and 2.0. All the packing density curves show "M" type with the minimum at $p = 1.0$ and two maximums at $p \approx 0.7, 2.0$.

curves show "M" type with various surface shape parameters. For the surface shape effects, the packing density curve is also in "M" type with various aspect ratios. Both slightly changing the surface shape and elongating (compressing) the particles will increase the random packing density. The effects of surface shape and aspect ratio are decoupled and the maximum of the random packing density is obtained at $p \approx 0.7, 2.0$ and $w \approx 0.7, 1.5$, as shown in Fig. 9, which demonstrates all the packing densities with different p and w in a map. Four maximums are observed in Fig. 9 at $p \approx 0.7$, $w \approx 0.7$; $p \approx 0.7$, $w \approx 1.5$; $p \approx 2.0$, $w \approx 0.7$ and $p \approx 2.0$, $w \approx 1.5$, respectively. The packing densities of the four maximums are all about 0.738. Additionally, the packing density of spheres ($p = 1.0, w = 1.0$) is a local minimum, which is consistent with the Ulam's conjecture [60] for random packings.

Moreover, we conjecture that the aspect ratio effects are applicable to all the symmetric particles with three equal main cross sections when $w = 1.0$, such as superballs, spherocylinders, truncated cubes, sphero-cubes and sphero-octahedra, of which all the three main cross sections are superdisks, disks, truncated square, rounded square and rounded rhombus, respectively. If these particles are compressed or elongated in one main direction, the maximum random packing density will be obtained when the uniaxial aspect ratio $w \approx 0.7, 1.5$, which will be verified in the future work.

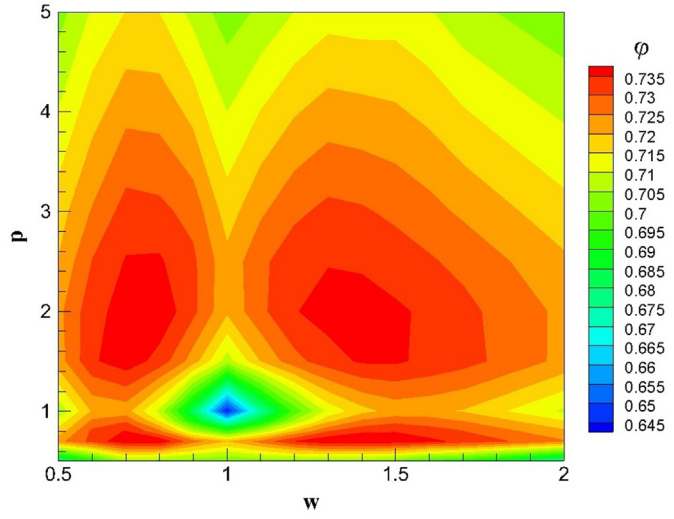

Fig. 9. The packing density map of superellipsoids for different surface shape parameter p and aspect ratio w.

3.3. The Voronoi analysis

In recent years, the Voronoi analysis [45] of non-spherical particle packings has become a standard means for structural analysis. The Voronoi channel method [66], the space discretization method [67–69] and the set Voronoi diagram method [70–72] are successfully developed to carry out the Voronoi tessellation of non-spherical particle packings. In this work, the set Voronoi diagram method is used to tessellate the superellipsoid packings and investigate the microcosmic properties of superellipsoid packings. In the set Voronoi diagram method, the surface of each particle is discretized into point sets. Then the Voronoi cells of all the discrete points are computed. Finally, the Voronoi cell of each particle is united by its own point sets. More details about the set Voronoi diagram method can be found in ref. [72]. Here we discretize the particle surface via the polar coordinates and the Voro++ program [73] is used to compute the Voronoi cells of discrete points. We investigate the Voronoi cell volume of particles via the reduced local Voronoi cell volume V_{local} which is defined as

$$V_{local} = \frac{V_{cell}}{V_p} \tag{16}$$

where V_p is the volume of the inner particle and V_{cell} is the volume of the particle's Voronoi cell. Here we use the reduced local Voronoi cell volume V_{local} rather than the local packing density, because the mean of V_{local} is accurately equal to the inverse of the global packing density φ.

A superellipsoid ($p = 2.5, w = 1.0$) surface discretized by 2246 points which are used to compute the Voronoi cells of particles is shown in fig. 10(a). The polar and azimuthal angles of these points are uniformly distributed. More points are distributed near the corners and edges, which are helpful to improve the accuracy. Fig. 10(b) shows the probability distribution of the reduced Voronoi cell volumes V_{local} in a MDRP of superellipsoids with $p = 2.5$, $w = 1.0$. The data are fitted by a Gaussian distribution function with a correlation factor $R^2 = 0.997$. The mean V^{μ}_{local} and standard deviation V^{σ}_{local} are 1.390 and 0.064, respectively. We note that all the probability distributions of V_{local} for different p and ω are in Gaussian distributions.

The accuracy of the set Voronoi diagram method depends on the number of discretized points and the particle shapes. The number of points used to discretize the superellipsoid surface is called the resolution [71]. The higher the resolution is, the more accurate the Voronoi cells will be. Fig. 10(c) shows the relative errors of the V^{σ}_{local} as a function of the resolution. Here five typical MDRPs of superellipsoids, which contains the sphere and four extreme shaped superellipsoids studied in this work, are used to validate the resolution. The relative errors of V^{σ}_{local} decrease rapidly with the increase of the resolution, and the errors are generally smaller than 3.0% if 2246 points are used. However, the computational cost increases rapidly as the resolution increases. As a compromise between accuracy and computational cost, we use 2246 points to discrete the surfaces of all the superellipsoids studied in this work.

The relationship between the V^{σ}_{local} and V^{μ}_{local} are shown in Fig. 10(d). When p is equal to 1.0, the superellipsoids degenerate to ellipsoids and a linear relationship is found between the V^{σ}_{local} and $V^{\mu}_{local} = 1/\varphi$, which means that the standard deviation of the reduced local Voronoi cell volume depends only on the global packing density of random ellipsoid packings. This phenomenon is also shown in ref. [69, 70], and was used to investigate the relationship between the average number of contacts and the global packing density in a random packing. Moreover, the V^{σ}_{local} and V^{μ}_{local} are in the same linear relationship when p is smaller

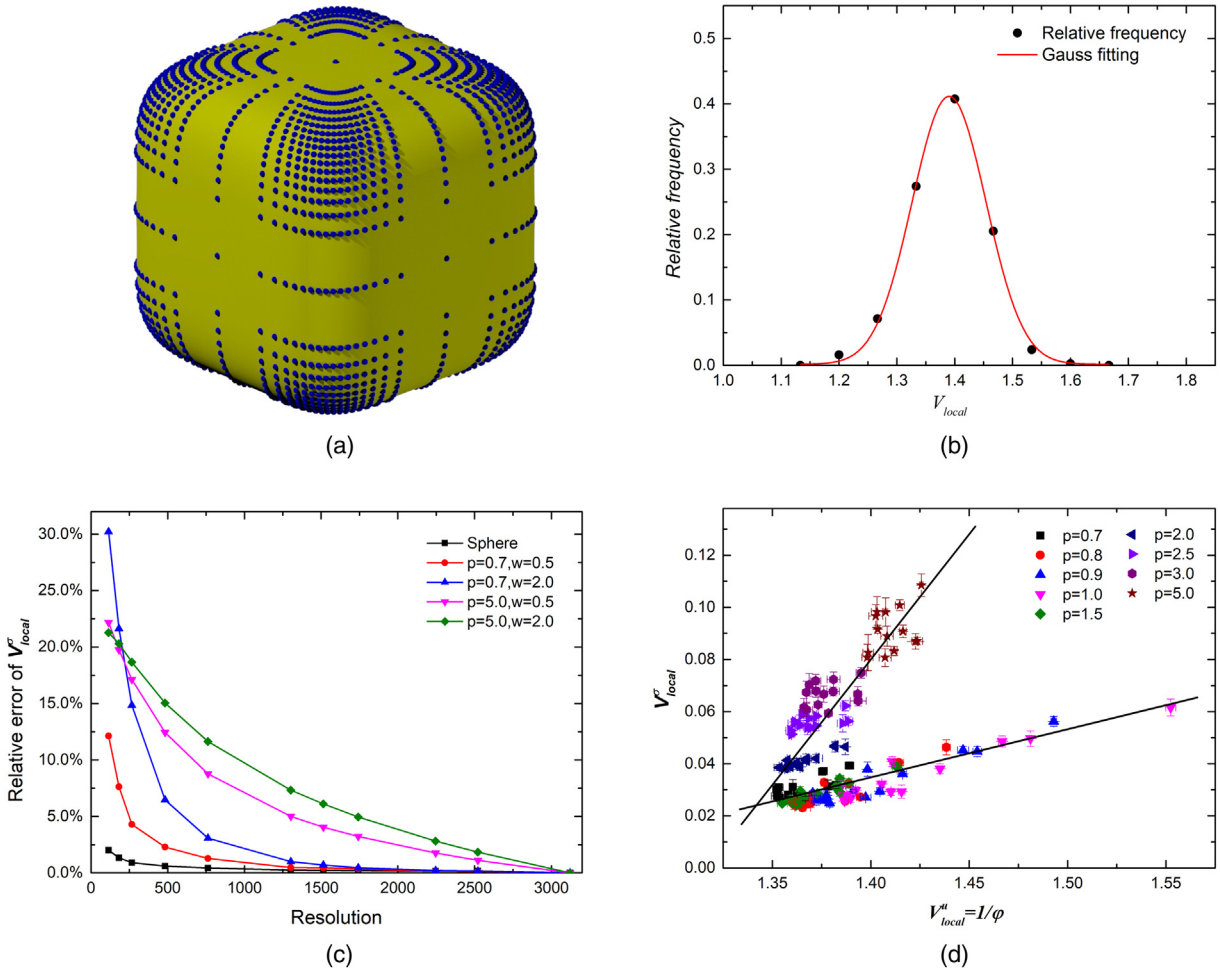

Fig. 10. (a) A superellipsoid ($p = 2.5, w = 1.0$) surface (yellow) discretized by 2246 points (blue) which are used to compute the Voronoi cells of particles. (b) The probability distribution of the reduced Voronoi cell volumes V_{local} in a MDRP packing of superellipsoids with $p = 2.5, w = 1.0$. The data are fitted by a Gaussian distribution function with a correlation factor $R^2 = 0.997$. (c) The relative errors of the V^{σ}_{local} as a function of the resolution. The MDRPs of spheres and four extreme shaped superellipsoids studied in this work are used to validate the resolution. (d) The relationship between the mean V^{μ}_{local} and standard deviation V^{σ}_{local} calculated from the packing configurations of superellipsoids with different p and w. The error bars are averaged over four times. Two linear relationships are observed.

than 1.5 regardless of the aspect ratios. However, another linear relationship is found when p is larger than 2.0 for different aspect ratios. Therefore, the linear relationship between the standard deviation of the reduced local Voronoi cell volume and the inverse of global packing density is not always the same, and is influenced by the particle surface shape parameter.

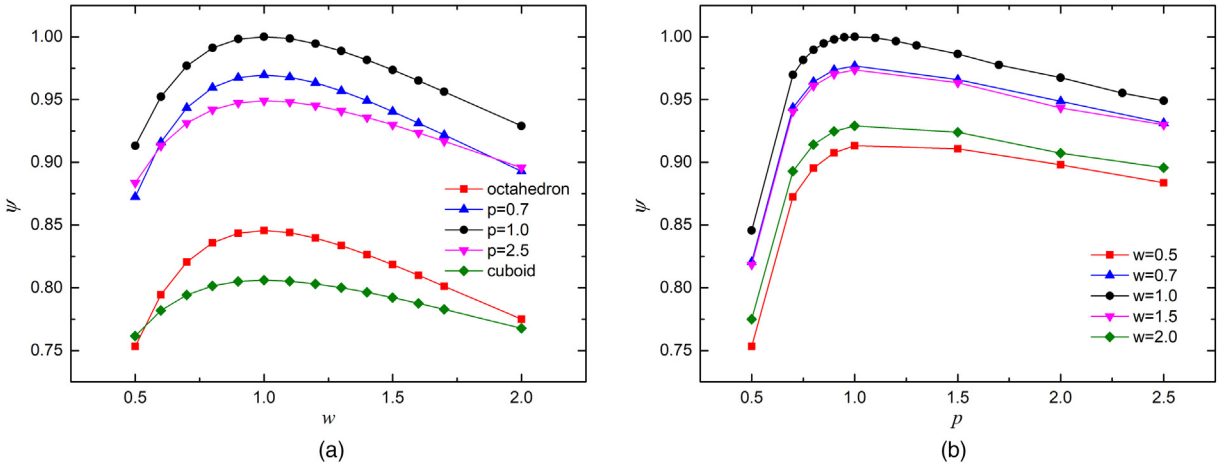

Fig. 11. The sphericities of the superellipsoids studied in this work. (a) The relationship between the sphericity ψ and aspect ratio w of superellipsoids for different surface shape parameter p. (b) The relationship between the sphericity ψ and surface shape parameter p of superellipsoids for different aspect ratio w.

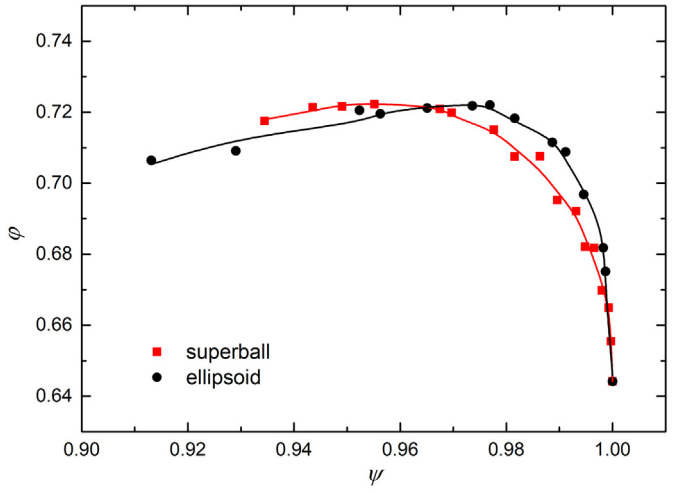

Fig. 12. The relationships between the packing density φ and the sphericity ψ for superballs ($w = 1.0$) and ellipsoids ($p = 1.0$).

3.4. The sphericities of superellipsoids

The sphericity, defined by Wadell in 1935 [74], is one of the most commonly used parameters in describing the shape of a particle [75]. The sphericity ψ is defined as the ratio of the surface area of a sphere which has the same volume as the given particle to the surface area of that particle.

$$\psi = \frac{\pi^{\frac{1}{3}}(6V_p)^{\frac{2}{3}}}{S_p} \tag{17}$$

where V_p and S_p are the volume and surface area of a particle, respectively. We calculate the sphericities of the superellipsoids studied in this work. Fig. 11(a) shows the relationship between the sphericity ψ and aspect ratio w of superellipsoids for different surface shape parameter p. The ψ reaches the maximum at $w = 1.0$ for different p. Meanwhile, the ψ reaches the maximum at $p = 1.0$ for different w, as shown in Fig. 11(b).

Fig. 12 shows the relationships between the sphericity ψ and packing density φ for superballs and ellipsoids. The surface shape parameter p ranges from 0.7 to 3.0. The $\varphi - \psi$ curve is uniform for superballs with $p > 1.0$ and $p < 1.0$, which means that the "M" typed packing density curve of superballs in Fig. 6 is folded into a single-peaked curve with the abscissa changed from p into ψ. In other words, the surface shape effects on the random packing density of superballs are equivalent if they have the same sphericity. The $\varphi - \psi$ curve is also uniform for ellipsoids ($p = 1.0$) with $w > 1.0$ and $w < 1.0$, meaning that the "M" typed packing density curve of ellipsoids with $p = 1.0$ in Fig. 7(a) and (b) is also folded into a single-peaked curve with the abscissa changed from w into ψ. Meanwhile, the "M" typed packing density curves of superellipsoids with $0.7 \le p \le 2.5$ in Fig. 7(a) and (b) are folded into single-peaked curves with the abscissa changed from w into ψ, which are shown in Fig. 13 (a) and (b). Therefore, the compressed and elongated aspect ratio effects on the random packing density of superellipsoids are also equivalent if they have the same sphericity. Moreover, the $\varphi - \psi$ curves with $0.7 \le p \le 2.5$ are almost in the same type.

To summarize, the surface shape effects on the random packing density of superballs are equivalent if they have the same sphericity. The compressed and elongated aspect ratio effects on the random packing density of superellipsoids are also equivalent if they have the same sphericity.

4. Conclusion

In this work, the MDRPs of superellipsoids are generated via the inverse Monte Carlo packing method. The normalized local cubatic order parameter and a new normalized local bond-orientational order parameter are used to evaluate the order degrees of orientations and bond-orientations, respectively. We obtain the MDRPs of superellipsoids with a wider range of the surface shape parameter. All the superellipsoid packings we generated are in the same random state and no obvious order structures exist. The MDRPs are more random with lower packing densities than literature results when the superellipsoids are close to ideal cubes. The local analyses of the MDRPs of superellipsoids are carried out via the Voronoi tessellation and two linear relationships between the mean and standard deviation of the reduced Voronoi cell volumes are obtained.

We find uniform and decoupled shape effects on the MDRPs of hard superellipsoids. Both slightly changing the surface shape and elongating (compressing) the particles will increase the random packing density. The influences of surface shape parameter p and aspect ratio w on the random packing densities are decoupled and the aspect ratio effects are applicable to all the symmetric particles with three same main cross sections when $w = 1.0$. The compressed and elongated aspect ratio effects on the random packing density of superellipsoids are equivalent if they have the same sphericity. For the aspect ratio effects, all the packing density curves show "M" type and do not change the type when p is varying. Meanwhile, for the surface shape effects, the packing

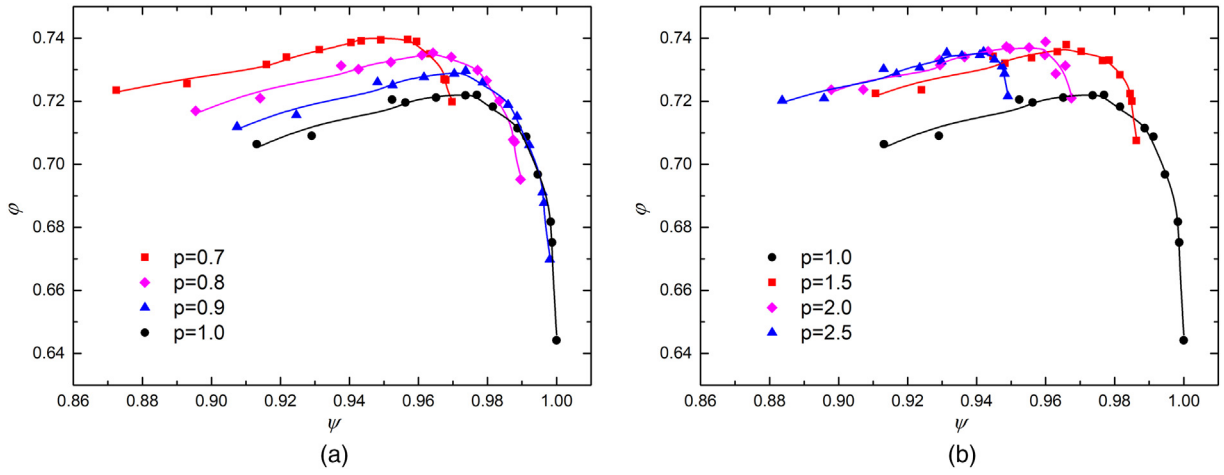

Fig. 13. The relationships between the packing density φ and the sphericity ψ for different superellipsoids. (a) Superellipsoids with the surface shape parameter $p = 0.7, 0.8, 0.9, 1.0$. (b) Superellipsoids with the surface shape parameter $p = 1.0, 1.5, 2.0, 2.5$.

density curve is also in "M" type and does not change the type when the aspect ratio varies. The maximum of the random packing density is obtained at $p \approx 0.7, 2.0$ and $w \approx 0.7, 1.5$ and the packing density of spheres is a local minimum.

The MDRP characterizes the onset of nontrivial spatial correlations among the particles and is a glass state of hard particle systems. Besides the states of RCP and MRJ, the MDRP state also provides a comparable random state for variously shaped particles. It has been applied to investigate the shape effects on the geometrical random packings under the same random conditions while the mechanical stability and jamming are not required. This is a fundamental problem and more MDRPs of particles with different shapes will be generated to conclude more general rules for surface shape and aspect ratio effects on random packings.

Moreover, the normalized local cubatic order parameter and the normalized local bond-orientational order parameter are applicable to other shaped particle packings to evaluate the order degree. The local Voronoi analysis demonstrates that the linear relationship between the standard deviation of the reduced local Voronoi cell volume and the inverse of global packing density is not always the same and is influenced by the particle surface shape parameter. Our results lead to a better understanding of the shape effects on random packings and are helpful in guiding the development of theoretical models for particle packings as well as the granular material design.

Acknowledgements

This work was supported by the National Natural Science Foundation of China (Grant No. 11272010, 11572004 and U1630112), the Science Challenge Project (Grant No. JCKY2016212A502) and the High-performance Computing Platform of Peking University.

References

[1] J.D. Bernal, J. Mason, Packing of spheres: co-ordination of randomly packed spheres, Nature 188 (1960) 910.
[2] G.D. Scott, K.R. Knight, J.D. Bernal, J. Mason, Radial distribution of the random close packing of equal spheres, Nature 194 (1962) 956.
[3] R. Zallen, The Physics of Amorphous Solids, Wiley, New York, 1983.
[4] S.F. Edwards, The role of entropy in the specification of a powder, in: A. Mehta (Ed.), Granular Matter, Springer, New York, 1994.
[5] P.M. Chaikin, T.C. Lubensky, Principles of Condensed Matter Physics, Cambridge University Press, New York, 2000.
[6] S. Torquato, Random Heterogeneous Materials: Microstructure and Macroscopic Properties, Springer-Verlag, New York, 2002.
[7] C.S. O'Hern, L.E. Silbert, A.J. Liu, S.R. Nagel, Jamming at zero temperature and zero applied stress: the epitome of disorder, Phys. Rev. E 68 (2003), 011306.
[8] A.J. Liu, S.R. Nagel, Nonlinear dynamics: jamming is not just cool any more, Nature 396 (1998) 21.
[9] S. Torquato, T.M. Truskett, P.G. Debenedetti, Is random close packing of spheres well defined? Phys. Rev. Lett. 84 (2000) 2064.
[10] S.R. Williams, A.P. Philipse, Random packings of spheres and spherocylinders simulated by mechanical contraction, Phys. Rev. E 67 (2003), 051301.
[11] C.R.A. Abreu, F.W. Tavares, M. Castier, Influence of particle shape on the packing and on the segregation of spherocylinders via Monte Carlo simulations, Powder Technol. 134 (2003) 167–180.
[12] X. Jia, M. Gan, Validation of a digital packing algorithm in predicting powder packing densities, Powder Technol. 174 (2007) 10–13.
[13] A. Wouterse, S.R. Williams, A.P. Philipse, Effect of particle shape on the density and microstructure of random packings, J. Phys. Condens. Matter 19 (2007) 406215.
[14] M. Bargiel, Geometrical properties of simulated packings of spherocylinders, Proceeding of 8th International Conference on Computational Science, vol. 5102, Springer-Verlag, Berlin 2008, pp. 126–135.
[15] P. Lu, S. Li, J. Zhao, L. Meng, A computational investigation on random packings of sphere-spherocylinder mixtures, Sci. China Phys. Mech. Astron. 53 (2010) 2284–2292.
[16] A.V. Kyrylyuk, M.A. van de Haar, L. Rossi, A. Wouterse, A.P. Philipse, Isochoric ideality in jammed random packings of non-spherical granular matter, Soft Matter 7 (2011) 1671–1674.
[17] J. Zhao, S. Li, R. Zou, A. Yu, Dense random packings of spherocylinders, Soft Matter 8 (2012) 1003–1009.
[18] C.F. Córdova, J.S.V. Duijneveldt, Random packing of hard spherocylinders, J. Chem. Eng. Data 59 (2014) 3055–3060.
[19] L. Meng, Y. Jiao, S. Li, Maximally dense random packings of spherocylinders, Powder Technol. 292 (2016) 176–185.
[20] A. Donev, I. Cisse, D. Sachs, E.A. Variano, F.H. Stillinger, R. Connelly, S. Torquato, P.M. Chaikin, Improving the density of jammed disordered packings using ellipsoids, Science 303 (2004) 990–993.
[21] P.M. Chaikin, A. Donev, W. Man, F.H. Stillinger, S. Torquato, Some observations on the random packing of hard ellipsoids, Ind. Eng. Chem. Res. 45 (2006) 6960–6965.
[22] A. Donev, R. Connelly, F.H. Stillinger, S. Torquato, Underconstrained jammed packings of nonspherical hard particles: ellipses and ellipsoids, Phys. Rev. E 75 (2007), 051304.
[23] X. Jia, R. Caulkin, R.A. Williams, Z. Zhou, A. Yu, The role of geometric constraints in random packing of non-spherical particles, Europhys. Lett. 92 (2010) 68005.
[24] G.W. Delaney, P.W. Cleary, The packing properties of superellipsoids, Europhys. Lett. 89 (2010) 34002.
[25] Z. Zhou, R. Zou, D. Pinson, A. Yu, Dynamic simulation of the packing of ellipsoidal particles, Ind. Eng. Chem. Res. 50 (2011) 9787–9798.
[26] K. Dong, C. Wang, A. Yu, Voronoi analysis of the packings of non-spherical particles, Chem. Eng. Sci. 153 (2016) 330–343.
[27] S. Zhao, N. Zhang, X. Zhou, L. Zhang, Particle shape effects on fabric of granular random packing, Powder Technol. 310 (2017) 175–186.
[28] Y. Jiao, F.H. Stillinger, S. Torquato, Distinctive features arising in maximally random jammed packings of superballs, Phys. Rev. E 81 (2010), 041304.
[29] A.H. Barr, Superquadrics and angle-preserving transformations, IEEE Comput. Graph. Appl. 1 (1981) 11–23.
[30] J.R. Williams, A.P. Pentland, Superquadrics and modal dynamics for discrete elements in interactive design, Eng. Comput. 9 (1992) 115–127.
[31] W. Zhong, A. Yu, X. Liu, Z. Tong, H. Zhang, DEM/CFD-DEM modelling of non-spherical particulate systems: theoretical developments and applications, Powder Technol. 302 (2016) 108–152.
[32] M. Kodam, R. Bharadwaj, J. Curtis, B. Hancock, C. Wassgren, Cylindrical object contact detection for use in discrete element method simulations. Part I–contact detection algorithms, Chem. Eng. Sci. 65 (2010) 5852–5862.
[33] T.C. Hales, A proof of the Kepler conjecture, Ann. Math. 162 (2005) 1065–1185.
[34] A. Donev, F.H. Stillinger, P.M. Chaikin, S. Torquato, Unusually dense crystal packings of ellipsoids, Phys. Rev. Lett. 92 (2004) 255506.
[35] W. Jin, Y. Jiao, L. Liu, Y. Yuan, S. Li, Dense crystalline packings of ellipsoids, Phys. Rev. E 95 (2017), 033003.
[36] Y. Jiao, F.H. Stillinger, S. Torquato, Optimal packings of superballs, Phys. Rev. E 79 (2009), 041309.
[37] R.D. Batten, F.H. Stillinger, S. Torquato, Phase behavior of colloidal superballs: shape interpolation from spheres to cubes, Phys. Rev. E 81 (2010), 061105.
[38] R. Ni, A.P. Gantapara, J. de Graaf, R. van Roij, M. Dijkstra, Phase diagram of colloidal hard superballs: from cubes via spheres to octahedra, Soft Matter 8 (2012) 8826–8834.
[39] D. Frenkel, B.M. Mulder, J.P. Mctague, Phase diagram of a system of hard ellipsoids, Phys. Rev. Lett. 52 (1984) 287–290.
[40] P.J. Camp, C.P. Mason, M.P. Allen, The isotropic–nematic phase transition in uniaxial hard ellipsoid fluids: coexistence data and the approach to the Onsager limit, J. Chem. Phys. 105 (1996) 2837.
[41] G. Bautista-Carbajal, A. Moncho-Jordá, G. Odriozola, Further details on the phase diagram of hard ellipsoids of revolution, J. Chem. Phys. 138 (2013), 064501.
[42] P.J. Camp, M.P. Allen, Phase diagram of the hard biaxial ellipsoid fluid, J. Chem. Phys. 106 (1997) 6681.
[43] L. Liu, P. Lu, L. Meng, W. Jin, S. Li, Order metrics and order maps of octahedron packings, Physica A 444 (2016) 870–882.
[44] L. Liu, Z. Li, Y. Jiao, S. Li, Maximally dense random packings of cubes and cuboids via a novel inverse packing method, Soft Matter 13 (2017) 748–757.
[45] G.F. Voronoi, J. Reine Angew. Math. 136 (1909) 67.
[46] J.W. Perram, M. Wertheim, Statistical mechanics of hard ellipsoids. I. Overlap algorithm and the contact function, J. Comput. Phys. 58 (1985) 409–416.
[47] A. Donev, Jammed Packings of Hard Particles, Princeton University, 2006 (PhD thesis).
[48] S. Li, P. Lu, W. Jin, L. Meng, Quasi-random packing of tetrahedra, Soft Matter 9 (2013) 9298–9302.
[49] P.J. Steinhardt, D.R. Nelson, M. Ronchetti, Bond-orientational order in liquids and glasses, Phys. Rev. B 28 (1983) 784.
[50] A.V. Mokshin, J.L. Barrat, Shear induced structural ordering of a model metallic glass, J. Chem. Phys. 130 (2009), 034502.
[51] H. Tanaka, T. Kawasaki, H. Shintani, K. Watanabe, Critical-like behaviour of glass-forming liquids, Nat. Mater. 9 (2010) 324.
[52] A. Ikeda, K. Miyazaki, Glass transition of the monodisperse Gaussian core model, Phys. Rev. Lett. 106 (2011), 015701.
[53] J.S.V. Duijneveldt, D. Frenkel, Computer simulation study of free energy barriers in crystal nucleation, J. Chem. Phys. 96 (1992) 4655.
[54] A.S. Keys, S.C. Glotzer, How do quasicrystals grow? Phys. Rev. Lett. 99 (2007) 235503.
[55] R. Ni, M. Dijkstra, Crystal nucleation of colloidal hard dumbbells, J. Chem. Phys. 134 (2011), 034501.
[56] A.R. Kansal, S. Torquato, F.H. Stillinger, Diversity of order and densities in jammed hard-particle packings, Phys. Rev. E 66 (2002), 041109.
[57] W. Mickel, S.C. Kapfer, G.E. Schröder-Turk, K. Mecke, Shortcomings of the bond orientational order parameters for the analysis of disordered particulate matter, J. Chem. Phys. 138 (2013), 044501.
[58] S. Torquato, Y. Jiao, Dense packings of polyhedra: Platonic and Archimedean solids, Phys. Rev. E 80 (2009), 041104.
[59] S. Torquato, Y. Jiao, Dense packings of the Platonic and Archimedean solids, Nature 460 (2009) 876–879.
[60] Y. Jiao, S. Torquato, Maximally random jammed packings of Platonic solids: Hyperuniform long-range correlations and isostaticity, Phys. Rev. E 84 (2011), 041309.
[61] K.C. Smith, I. Srivastava, T.S. Fisher, M. Alam, Variable-cell method for stress-controlled jamming of athermal, frictionless grains, Phys. Rev. E 89 (2014), 042203.

[62] J. Baker, A. Kudrolli, Maximum and minimum stable random packings of platonic solids, Phys. Rev. E 82 (2010), 061304.
[63] A.G. Athanassiadis, M.Z. Miskin, P. Kaplan, N. Rodenberg, S.H. Lee, J. Merritt, E. Brown, J. Amend, H. Lipsonb, H.M. Jaeger, Particle shape effects on the stress response of granular packings, Soft Matter 10 (2014) 48–59.
[64] A. Baule, F. Morone, H.J. Herrmann, H.A. Makse, Edwards statistical mechanics for jammed granular matter, Rev. Mod. Phys. 90 (2018), 015006.
[65] B.D. Lubachevsky, F.H. Stillinger, Geometric properties of random disk packings, J. Stat. Phys. 60 (1990) 561–583.
[66] V.A. Luchnikov, N.N. Medvedev, L. Oger, J.P. Troadec, Voronoi-Delaunay analysis of voids in systems of nonspherical particles, Phys. Rev. E 59 (1999) 7205–7212.
[67] R. Al-Raoush, K.A. Alshibli, Distribution of local void ratio in porous media systems from 3D X-ray microtomography images, Physica A 361 (2006) 441–456.
[68] C. Xia, K. Zhu, Y. Cao, H. Sun, B. Kou, Y. Wang, X-ray tomography study of the random packing structure of ellipsoids, Soft Matter 10 (2014) 990.
[69] K. Dong, C. Wang, A. Yu, Voronoi analysis of the packings of non-spherical particles, Chem. Eng. Sci. 153 (2016) 330–343.
[70] F.M. Schaller, M. Neudecker, M. Saadatfar, G.W. Delaney, G.E. Schröder-Turk, M. Schröter, Local origin of global contact numbers in frictional ellipsoid packings, Phys. Rev. Lett. 114 (2015) 158001.
[71] S. Zhao, T.M. Evans, X. Zhou, Three-dimensional Voronoi analysis of monodisperse ellipsoids during triaxial shear, Powder Technol. 323 (2018) 323–336.
[72] F.M. Schaller, S.C. Kapfer, M.E. Evans, M.J.F. Hoffmann, T. Aste, M. Saadatfar, K. Mecke, G.W. Delaney, G.E. Schröder-Turk, Set Voronoi diagrams of 3D assemblies of aspherical particles, Philos. Mag. 93 (2013) 3993–4017.
[73] C.H. Rycroft, Voro++: a three-dimensional Voronoi cell library in C++, Chaos 19 (2009), 041111.
[74] H. Wadell, Volume, shape, and roundness of quartz particles, J. Geol. 43 (1935) 250–280.
[75] R. Zou, A. Yu, Evaluation of the packing characteristics of mono-sized non-spherical particles, Powder Technol. 88 (1996) 71–79.